Fully Digital Horus Radar Experiments in Support of DARPA's Beyond Linear Processing Program

Mark Yeary[1,2], David Schvartzman[1,2,3], Matthew Herndon[1,2], Robert D. Palmer[1,2,3], Benjamin Epstein[4], Frank Robey[5]

[1]*Advanced Radar Research Center* (ARRC), *The* University *of* Oklahoma
[2]*School of Electrical and Computer Engineering*, *The* University *of* Oklahoma
[3]*School of Meteorology*, *The* University *of* Oklahoma
[4]*ECS Federal*
[5]*Defense Advanced Research Projects Agency* (DARPA)

2024 IEEE International Symposium on Phased Array Systems and Technology (ARRAY) | 979-8-3503-9214-2/24/$31.00 ©2024 IEEE | DOI: 10.1109/ARRAY58370.2024.10880425

***Abstract*—In support of DARPA's Beyond Linear Processing (BLiP) Program, a team of several organizations deployed the University of Oklahoma ARRC's fully-digital Horus radar for a series of coordinated experiments that took place in the Winter 2024. Experiments were conducted with an instrumented Learjet aircraft from Phoenix Air, flying prescribed flight profiles. One of the key goals in the BLiP program is to evaluate the performance of aircraft tracking as a function of reduced aperture configurations. To this end, each prescribed flight path was repeated 3 times, and the Horus aperture was reconfigured to 100%, 75%, and 50% for each of the flights. The scans included uniform and staggered pulse-repetition time sequences, to evaluate Doppler estimation performance. This paper provides an overview of the instruments, the data collection activities, and the advanced beamforming scan modes exercised by the Horus radar.**

***Index Terms*—phased array radar, digital radar, aircraft tracking, beamforming**

I. Introduction

As phased array radar technology migrates to digital technology, these radars offer excellent benefits to advanced scanning and array processing capabilities, for example [1], [2], [3], [4], [5], [6]. Yet, fully digital architectures offer the maximum in flexibility, for instance [7], [8], [9], [10], etc. In such architectures, every element and polarization has its own transmitter and receiver and is usually quite flexible in terms of software reconfigurability. In collaboration with the Defense Advanced Research Projects Agency (DARPA), several organizations have recently conducted coordinated experiments between the fully digital "Horus" radar [9] in Fig. 1 and a Learjet aircraft from Phoenix Air Aviation Services. Organizations supporting DARPA as part of the Government Team include MIT-Lincoln Laboratory, Georgia Tech Research Institute (GTRI), Johns Hopkins University Applied Physics Laboratory (JHU-APL), and the University of Oklahoma (OU) Advanced Radar Research Center (ARRC).

Fig. 1. The fully digital Horus phased array radar, deployed for the BLiP experiments at The University of Oklahoma.

Experiments were conducted with the Horus radar in support of DARPA's Beyond Linear Processing (BLiP) program in January 2024. The experiments took place in Norman, OK, where the Horus radar is regularly deployed. A total of five flight profiles were designed to test aircraft detection using advanced digital beamforming capabilities. Each profile was conducted three times using different transmit/receive aperture configurations. These include a full aperture (100%), a 75%, and a 50% configuration, which represent the percentage of antenna elements used to transmit/receive beams. The reduced aperture configurations are intended to evaluate aircraft tracking performance in comparison to the full aperture case.

This research was developed with funding from the Defense Advanced Research Projects Agency (DARPA). The Horus-NOAA radar development was supported by the NOAA National Severe Storms Laboratory under NOAA-University of Oklahoma Cooperative Agreement #NA11OAR4320072, U.S. Department of Commerce. This material is also based upon research supported by, or in part by, the U. S. Office of Naval Research under award numbers N00014-18-1-2896, N00014-19-1-2326, N00014-20-1-2851, N00014-23-1-2762. Distribution Statement "A" (Approved for Public Release, Distribution Unlimited).

II. Beyond Linear Processing

The Beyond Linear Processing (BLiP) program [11], initiated by DARPA, aims to enhance radar performance through the application of innovative signal processing methods. Radar signal processing has evolved incrementally from processing in analog circuits to digital hardware implementation, firmware, and now implementation in software. Linear processing of the signal from the antenna to the detector has been retained in this evolution. The tremendous increase in processing capability enables a fresh look into radar signal processing. BLiP is based on the premise that when more physically realistic target and environment models are used as the basis for the radar estimation and detection problem, then solutions require non-linear and iterative signal processing [11]. Non-linear and iterative techniques have the potential to significantly improve radar performance such that smaller radar apertures and thus smaller platforms can provide equivalent capability, leveraging current high-power computer processing [11]. For example, non-linear algorithms such as compressive sensing, iterative algorithms, supervised / unsupervised learning, advanced dimensionality reduction techniques, and non-linear state estimation approaches (e.g., particle filtering) are important in modeling signal, clutter, and noise spaces for non-linear processing (e.g., [12], [13], [14], [15], [16], [17], [18], etc.). Non-linear and iterative techniques advancements could result in radar systems that are lighter, smaller, and less expensive, while maintaining the same level of capability [11]. For the first time, fully digital arrays have the flexibility to support these concepts. If successful, BLiP would enable the radar performance currently achieved on large platforms to be realized on much smaller sea, air, and ground platforms [11]. Over the course of this program [11], end-to-end radar signal processing chains are being developed, analyzed, implemented and tested; initially through non-real-time laboratory testing and culminating in real-time implementation and full-scale field testing.

III. Instruments

A. The Fully Digital Horus Radar

Horus is based on the most advanced PAR architecture, a fully digital design enabled by the ADI9371 RF transceiver. In this system, every element and polarization has its own transmitter and receiver to provide maximum flexibility in terms of beamforming and software reconfigurability. This radar is considered an *engineering* demonstrator with the goal of mitigating risks associated with fully digital phased array architectures and demonstrating advanced capabilities. Its size and operating frequency (see Table I) limit the beamwidth to $\sim$3.5° (i.e., with taper), which is not adequate to resolve complex structures in most severe weather precipitation systems that are far from the radar. However, its inherent scalable design allows the demonstration of overall functionality while considering plans for future full-scale systems. More details about Horus can be found in [9].

B. Phoenix Air Learjet

The airborne component of the DARPA BLiP experiments were carried out with an instrumented Learjet 36A aircraft operated by the Phoenix Air Group. The Phoenix Air Group is a non-scheduled air charter that provides user-defined services including highly modified aircraft for special missions. Pilots from Phoenix Air supported the DARPA BLiP experiments, flying an instrumented Learjet 36A in predefined flight paths in south/central Oklahoma. Learjet 36A is a pressurized, twin-engined transport-category airplane originally marketed as light business and military transports. The airplane is certified with a service ceiling of 45,000 feet and a nominal cruise speed of Mach 0.77. During the experiments, the aircraft was operated at a constant indicated airspeed of 220 knots, with altitude varying between 2,750 feet above mean sea level (MSL) and 16,850 feet MSL. For instance, Fig. 3 depicts an example flight path from Profile 5.

IV. Data Collection Experiments

A series of tests were conducted over two days using the Horus radar to observe airborne targets, intentional interference and weather. The airborne targets included targets of opportunity such as commercial airline traffic as well as the aforementioned Phoenix Air Learjet 36A, which flew five different pre-defined flight profiles. Each profile was designed to challenge parts of the radar signal processing chain. Profile 1 was a detection range test intended to probe the boundary for first target detectability and track. This profile included multiple transponder returns at different range offsets and with varying effective radar cross section. The transponder returns are generated by receiving the radar signal, adding time delay, scaling and then transmitting the resulting signal toward the radar. Other teams will use these multiple moving target returns to understand their detection and track statistics, which would not otherwise be possible with a single aircraft run. Next, Profile 2 was a range resolution test meant to test for the minimum range that two targets could be distinguished. Profile 3 was a low altitude test intended to place the Learjet low on the horizon and in the same elevation beam as ground clutter. Profile 4 was intended to present the Learjet at low Doppler relative to the radar. Profile 5 was intended to present a maneuvering and crossing target. Each profile was conducted 3 times, once per array size and corresponding waveform and scan design for a total of 15 test points (see Fig. 2).

A. Horus Scans

To cover a large volume centering the Phoenix Air's designated flight path, a sector from -45° to 45° in azimuth and 0° to 20° in elevation (relative to the radar) was selected as the region of interest. To sample this space with the radar, a grid of 64 'primary' steers was designed using a 2D broadened beam on transmit. The primary steer represents the gradient applied to the transmit-side 2D broadened beam and the receive-side uniform pencil beam to steer to a specific azimuth / elevation position relative to the radar. To enable arbitrary receive imaging within the broadened transmit beam's illumination

Flight	Baseline Scan Design 100%	75% Array Size with Performers Scan	50% Array Size with Performers Scan
Profile 1 (Detection Range)	Test Point 1A	Test Point 1B	Test Point 1C
Profile 2 (Range Resolution)	Test Point 2A	Test Point 2B	Test Point 2C
Profile 3 (Clutter, Low Altitude)	Test Point 3A	Test Point 3B	Test Point 3C
Profile 4 (Low Doppler)	Test Point 4A	Test Point 4B	Test Point 4C
Profile 5 (Maneuver – S turn)	Test Point 5A	Test Point 5B	Test Point 5C

Fig. 2. Test matrix for the coordinated experiments.

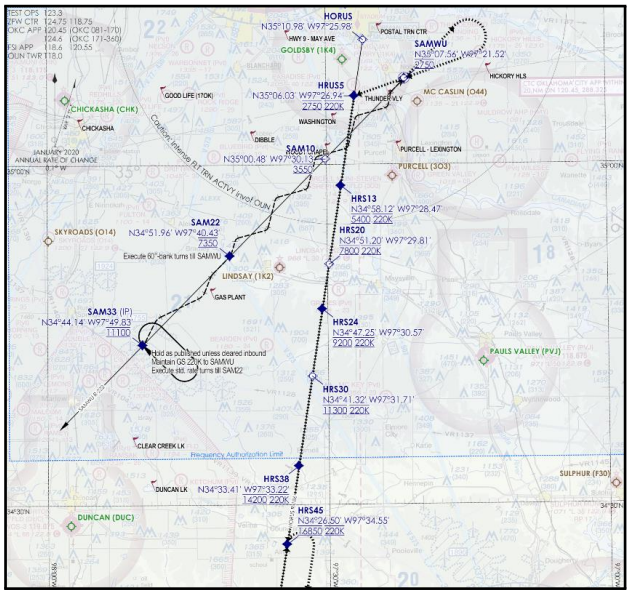

Fig. 3. Profile 5 prepared for the S-curve test.

region, the array's digital receivers were configured as 13 identical, non-overlapping digital subarrays with aperture sizes that varied by test case. Fig. 4 depicts the raster mechanism of the overall scan which was common across all test cases.

Beamforming coefficients for the broadened transmit patterns (i.e., 2D-spoiled transmit patterns) and the reduced aperture configurations were derived using a phase-only optimization framework [19]. For the BLiP experiment, these beams were designed to illuminate the same region in space for all array configurations (accounting for the aperture reduction). Particular emphasis was placed on the beam's mainlobe flatness during optimization. Transmit and receive beams for the three aperture size are presented in Fig. 5.

In terms of general radar scan parameters, some were changed and some were held constant between scans. For aperture case A, a single PRF of 1.35 kHz was used, while in aperture cases B and C a staggered PRF scheme was used with PRF1 1.5 kHz and PRF2 1.2 kHz. In both cases, these PRFs result in an overall scan time of 3.1 s per volume. Several parameters were also held constant across test cases to act as the baseline scan. The receiver was configured for 7.8125 MHz of baseband bandwidth with a range swath from 5 to 95 km (48.6 nmi). The system's overall data rate was also held constant at 1.5 Gbps.

B. Preliminary Results

By the end of the experiment, data from all flight profiles and array configurations had been captured. In total, 7 hours of data were captured during the flight tests corresponding to around 4.7 terabytes of digital subarray data, composed of a series of 3.1-s "frames" defined by the raster described in Section IV-A. Initial processing of the dataset was performed to verify returns from the experiment. A fine uniform grid of azimuth and elevation sampling points was formed from the coarse-raster subarray data using digital beamforming, allowing the full sector to be imaged in an intuitive way. Fig. 6 shows a single frame from test point 5A (see Fig. 2) visualizing these volumetric returns, noteworthy features include the strong weather returns and the target of opportunity flying across the scene. At this point within its flight profile, the Phoenix Air Learjet was flying within the weather clutter. These data were made available to the other participants in BLiP for further processing per the program's goals.

V. Conclusions

This paper describes the use of a unique radar for coordinated data collection experiments exercising advanced scanning modes. The radar utilized a runtime re-configurable broadended-beam digital subarray strategy to rapidly scan a large region of space, resulting in a volumetric dataset with many planned and unplanned targets and features. The team on this paper had responsibility for the overall execution of the data collection and in particular, worked to design the Horus array's scan strategy and parameters to meet hardware, software and experimental constraints prior to the experiment. Other teams will work to process the data, whereby advancements in non-linear and iterative signal processing methods are the primary goals.

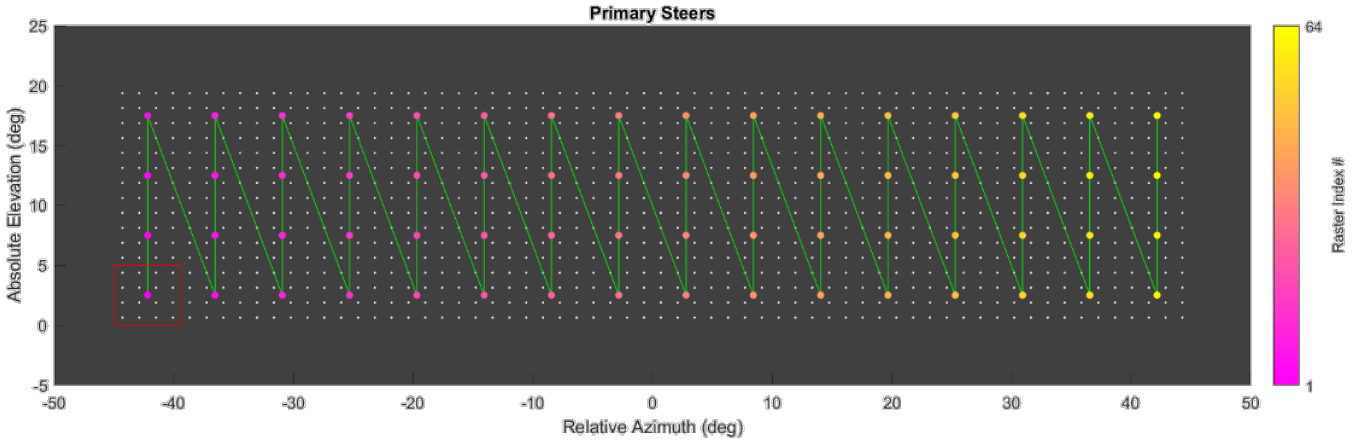

Fig. 4. Visualization of the scan strategy employed by the Horus-NOAA radar during the data collect. Each colored dot represents a primary steering position (colored with its corresponding raster index), with the red square roughly showing the region illuminated by the transmit beam. The remaining background dots represent 'secondary' steers formed via digital beamforming in post-processing. These correspond to the pixels produced in the top plot in Fig. 6.

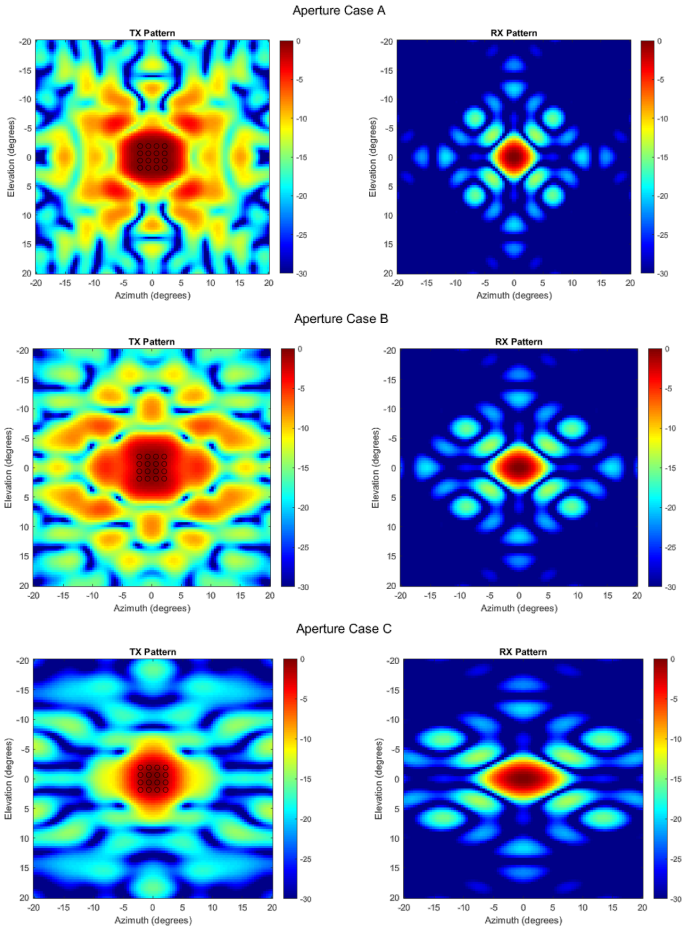

Fig. 5. Transmit (left) and receive (right) beam patterns for the full aperture (top row), 75% aperture (middle row), and 50% aperture (bottom row) configurations used. The 4×4 grid of dots in each TX pattern on the left correspond to the secondary steers surrounding each primary steer, contained within the red square in Fig. 4.

VI. Acknowledgment

Special thanks to the ARRC's engineering staff for their dedication to the project. The authors are grateful for Cameron Coupe from MIT-LL, Arthur Chu from MIT-LL, Aaron "Arho" Holdaway from GTRI, and Jim Perkins from GTRI for their assistance with the aircraft and experimental planning. We are appreciative of JHU-APL's Salvador Talisa for helping to verify the efficacy of the collected data during initial analysis. The views, opinions, and/or findings expressed are those of the author(s) and should not be interpreted as representing the official views or policies of the Department of Defense or the U.S. Government.

Appendix

TABLE I
Specifications of the Horus Radar

Frequency	S-band
Polarization	ATSR/STSR/RHCP/LHCP
Tx Waveform	Arbitrary Waveform Generator
Tx Peak Power (single element)	10 W/polarization
Max Tx Pulse Width	100 μs @ 10% duty cycle
Max Tx Bandwidth	100 MHz
Element Spacing	0.5 λ @ 2.951 GHz
Number of Populated Panels	13 (1664 total elements dual-pol)
Max Electronic Scan Angle	$\pm 45^\circ$ az, $\pm 45^\circ$ el
Aperture Size	2.03×2.03 m^2
Tx/Rx Beamwidth Broadside	2.58° (no taper)

References

[1] S. H. Talisa, K. W. O'Haver, T. M. Comberiate, M. D. Sharp, and O. F. Somerlock, "Benefits of digital phased array radars," *Proceedings of the IEEE*, vol. 104, no. 3, pp. 530–543, 2016.

[2] W. H. Weedon and R. D. Nunes, "Low-cost wideband digital receiver/exciter (DREX) technology enabling next-generation all-digital phased arrays," in *2016 IEEE International Symposium on Phased Array Systems and Technology (PAST)*. IEEE, 2016, pp. 1–5.

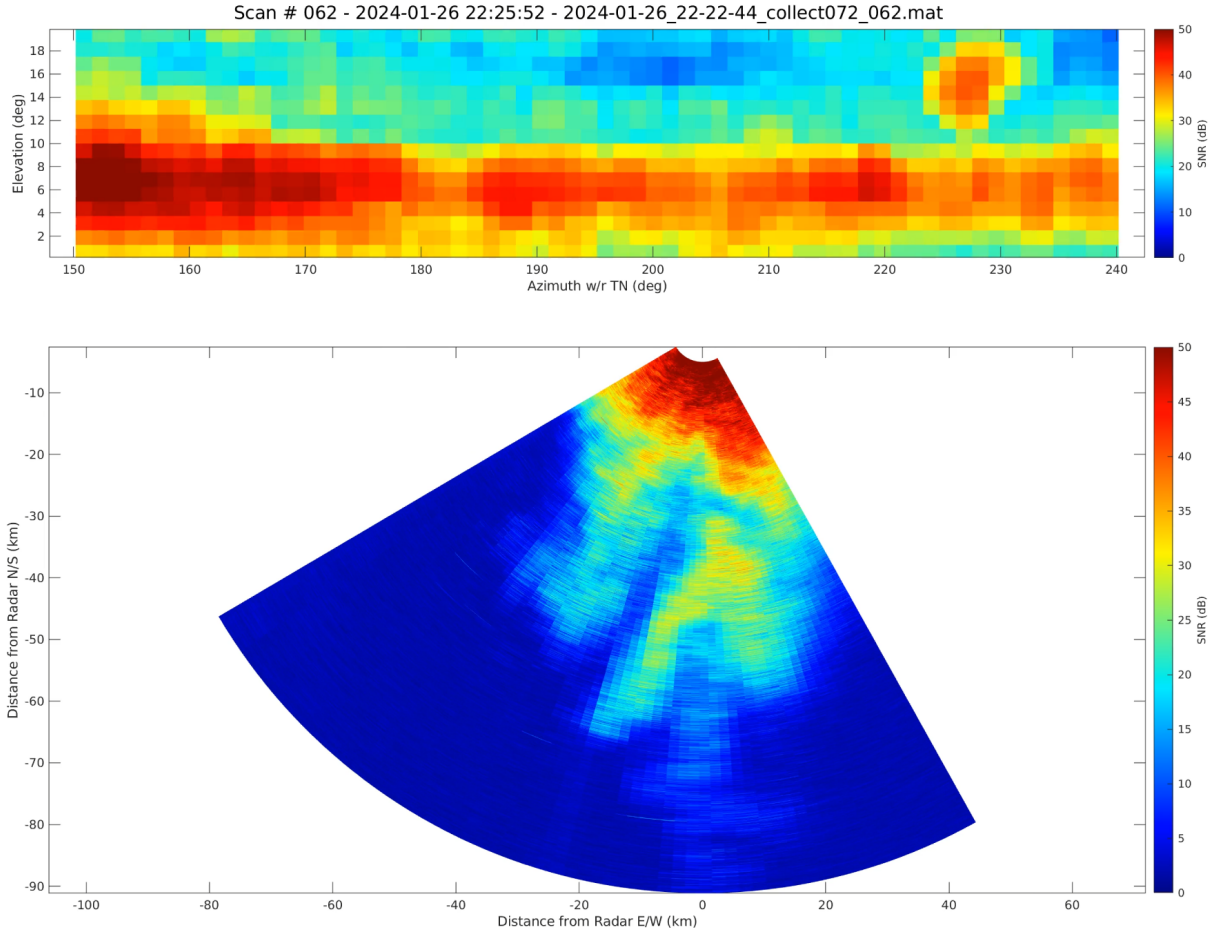

Fig. 6. Radar plot formed from volumetric Horus data showing targets of opportunity and widespread weather returns around the radar site. The top figure depicts the maximum energy observed downrange for each steering angle, while the bottom plot shows a PPI formed from the data.

[3] J. S. Herd and M. D. Conway, "The evolution to modern phased array architectures," *Proc. of the IEEE*, vol. 104, no. 3, pp. 519–529, 2015.

[4] D. J. Rabideau, R. J. Galejs, F. G. Willwerth, and D. S. McQueen, "An S-band digital array radar testbed," in *IEEE International Symposium on Phased Array Systems and Technology, 2003*. IEEE, 2003, pp. 113–118.

[5] K. Steiner and M. Yeary, "A 1.6 GHz sub-Nyquist-sampled wideband beamformer on an RFSoC," *IEEE Transactions on Radar Systems*, 2023.

[6] M. D. Conway, D. Du Russel, A. Morris, and C. Parry, "Multifunction phased array radar advanced technology demonstrator nearfield test results," in *2018 IEEE Radar Conference*. IEEE, 2018, pp. 1412–1415.

[7] J. A. Haimerl, B. Hudson, G. P. Fonder, and D. K. Lee, "Overview of the large digital arrays of the Space Fence radar," in *IEEE Intl. Symposium on Phased Array Systems and Technology*. IEEE, 2016, pp. 1–8.

[8] C. Fulton, R. Palmer, M. Yeary, J. Salazar, H. Sigmarsson, M. Weber, and A. Hedden, "Horus: A testbed for fully digital phased array radars," *Microwave Journal*, vol. 63, no. 1, pp. 20–36, 2020.

[9] R. D. Palmer, M. B. Yeary, D. Schvartzman, J. L. Salazar-Cerreno, C. Fulton, M. McCord, B. Cheong, D. Bodine, P. Kirstetter, H. Sigmarsson, T. Yu, D. Zrnic, R. Kelley, J. Meier, and M. Herndon, "Horus–a fully digital polarimetric phased array radar for next-generation weather observations," *IEEE Transactions on Radar Systems*, 2023.

[10] M. Yeary, R. Palmer, C. Fulton, J. Salazar, and H. Sigmarsson, "Update on an S-band all-digital mobile phased array radar," in *2021 IEEE Radar Conference (RadarConf21)*. IEEE, 2021, pp. 1–4.

[11] F. Robey, "DARPA BLiP Program," vol. HR001123S0008, pp. 1–33, 2022. [Online]. Available: https://www.darpa.mil/program/beyond-linear-processing

[12] I. Pitas and A. N. Venetsanopoulos, *Nonlinear Digital Filters: Principles and Applications*. Springer Science & Business Media, 2013, vol. 84.

[13] S. Stergiopoulos, *Advanced Signal Processing Handbook: Theory and Implementation for Radar, Sonar, and Medical Imaging Real Time Systems*. CRC Press, 2017.

[14] B. Harker, Z. Dobrosavljevic, E. Craney, C. Tubb, and G. Harris, "Dynamic range improvements and measurements in radar systems," *IET Radar, Sonar & Navigation*, vol. 1, no. 6, pp. 398–406, 2007.

[15] M. Rangaswamy, D. D. Weiner, and A. Ozturk, "Non-Gaussian random vector identification using spherically invariant random processes," *IEEE Trans. on Aero. and Elec. Systems*, vol. 29, no. 1, pp. 111–124, 1993.

[16] E. J. Kelly, "An adaptive detection algorithm," *IEEE Transactions on Aerospace and Electronic Systems*, no. 2, pp. 115–127, 1986.

[17] F. C. Robey, D. R. Fuhrmann, E. J. Kelly, and R. Nitzberg, "A CFAR adaptive matched filter detector," *IEEE Transactions on Aerospace and Electronic Systems*, vol. 28, no. 1, pp. 208–216, 1992.

[18] S. Kraut, L. L. Scharf, and L. T. McWhorter, "Adaptive subspace detectors," *IEEE Trans. on Signal Proc.*, vol. 49, no. 1, pp. 1–16, 2001.

[19] D. Schvartzman, R. D. Palmer, M. Herndon, and M. Yeary, "Pattern synthesis and digital beamforming capabilities of the fully digital Horus radar," in *IEEE Radar Conference*, 2024, pp. 01–06.